A Simple Estimation of Young's Modulus and Tensile Strength of Carbon Nanotubes

Debnarayan Jana[1]

[1]Department of Physics
University of Calcutta, 92 A P C Road
Kolkata 700 009, India.
E-mail: djphy@caluniv.ac.in

Abstract

Within the harmonic approximation, we estimate the Young's modulus and tensile strength of typical carbon nanotubes at zero temperature following four important potentials used in solid state physics. The theoretical results are compared with experimental observations. The results thus obtained also find an important link with the applicability of carbon nanotubes as a space elevator.

1. Introduction

Scientific discovery along with technological revolutions strongly depends on materials. To achieve smaller, faster and reliable smart devices for the continuing need of present age, it is highly essential to understand the properties of the materials in depth. Mechanical, optical properties of nano-structures [1,2] and nano particles coupled with electronic study are indeed one of the exciting fields of research from basic science. This study also forms the basis for future smart devices.

After Iijima's pioneering and illustrious work on carbon nanotubes [3] and single-walled carbon nanotubes (SWCNTs) [4–8] in the early 1990s sparked a general growing interest in fundamental condensed matter physics as well as nano science and nanotechnology. To describe the structures of SWCNT, one needs to know graphene, the basic building block of carbon allotropes.

Graphene is a one-atom-thick planar sheet of carbon atoms that is densely packed in a honeycomb crystal lattice. We show schematically in Fig. 1 the computer generated graphene and the direct image obtained by Meyer et al. [9] side by side. It is worthy to mention at this point that the graphene [6,10-12], by itself, can be characterized as either a zero-gap semiconductor or a metal (since the density of states (DOS) is zero at the Fermi energy (E_F)) and naturally, graphene imparts these properties to a nanotube.

Carbon nanotubes (CNTs) are the allotropes of carbon with a cylindrical nanostructure. Conceptually, CNTs are cylindrically shells made by rolling graphene sheets into a seamless cylinder. These sheets are rolled at specific and discrete angles. The typical length of a SWCNT can be between 1–100 μm and diameter around 1-10 nm. The perfect CNTs have crystalline structures formed by the hexagonal rings of benzene molecule with double and single C–C bonding. In Fig. 2, we schematically show the formation of SWCNT from graphene and fullerene. Their unique one dimensional structure with curvature in the sidewall is one of the

paradigms in the low dimensional systems of inter-disciplinary research.
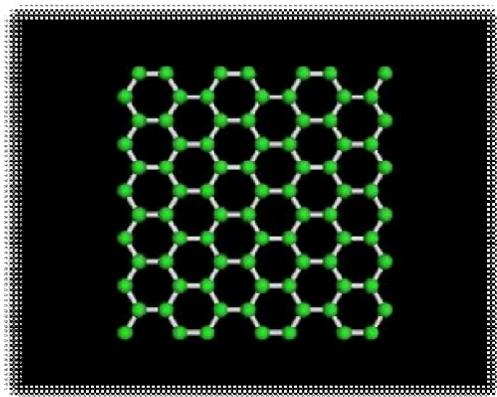
(a)
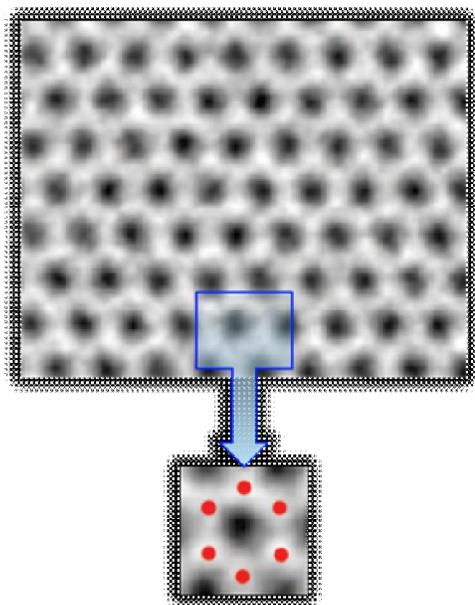
(b)

Fig. 1. (a) Computer generated graphene visual showing the honeycomb lattice structure. (b) Direct image of a single-layer graphene membrane (Red dots denote carbon atoms)

The typical molecular structure of SWCNTs can be characterized by a chiral circumferential vector $\vec{AB} = n\vec{a} + m\vec{b}$, a linear combination of two

unit lattice vectors *a* and *b* with *m* and *n* being integers. The pair of indices *(n,m)* for any given nanotube structure determines its diameter, chirality, and the basic electronic character.

For example, if *n = m*, the nanotube is designated as armchair and is metallic in nature (with a zero bandgap, strictly speaking). While for n ≠ m and neither *n* nor *m* are zero, the CNT exhibits chirality, having important implications in optical properties.
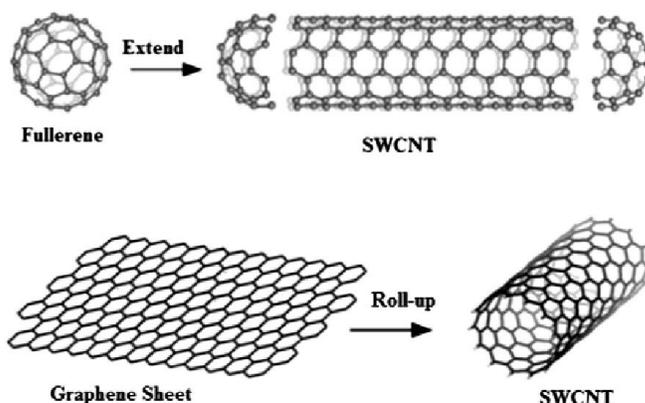

Fig. 2. Schematic illustration of formation of SWCNT from Fullerene and graphene sheet

For *n = 0* or *m = 0*, the CNT is termed zigzag. If $n - m \neq 3p$, where *p* is a non-zero integer, the CNT is semimetallic/ quasi-metallic with a band gap of the order of meV. For $n - m = 3p$, where *p* is a non-zero integer, the CNT is semi-conducting having a band gap of the order of 1 eV. In fig. 3, the various flavors of CNTs are illustrated through the chiral circumferential vector. From the circumferential vector AB, one can easily obtain the diameter and chiral angle, the characteristic features of a typical CNT.

The diameter of a given nanotube can be expressed in terms of (n,m) and the carbon–carbon bond length 0.142 nm. The typical geometry of simple hexagonal unit used in generating the structures of CNT or graphene is shown in Fig. 4.

The distance (*a*) between two carbon atoms as shown in Fig. 4 is 0.142 nm while the half distance between any two parallel bonds ($b/2 = (\sqrt{3} \times 0.142)/2$ nm=0.123 nm). The diameter of a given nanotube can be expressed [1,4] in terms of (*n,m*) as

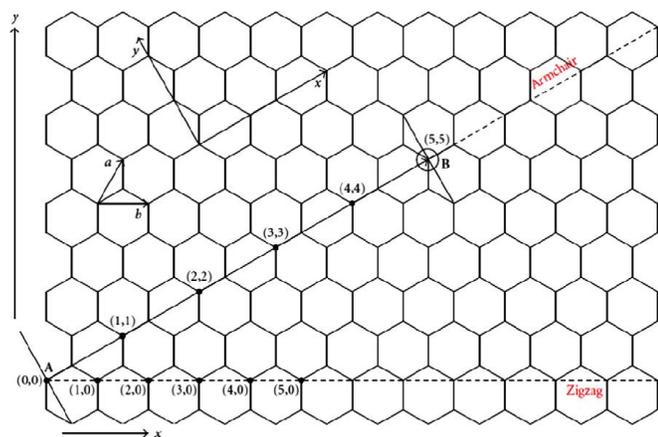$$d_{nm} = \frac{\sqrt{3} \times 0.142}{\pi} \sqrt{n^2 + nm + m^2} \ .$$

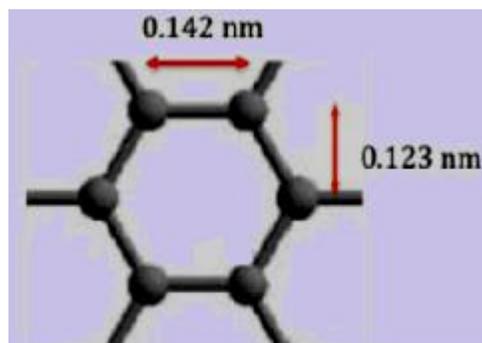**Fig.** 3. Schematic illustration of various carbon nanotubes

Fig. 4 A Typical hexagonal unit for formation of graphene

C-G bonds are one of the strongest bonds in nature. It has been illustrated in Fig 3 and 4 that the carbon nanotube is composed of perfect arrangement of these bonds. Because of these bonds, carbon nanotubes are the strongest material [1,4] known ever having Young's modulus (*Y*)

1250 GPa and tensile strength (σ) 11-63 GPa quite comparable to diamond. In comparison, the values of *Y* and σ in steel are 200 GPa and 2 GPa respectively. In this paper, we would like to present a simple model calculation to estimate the high values of Y and σ. In table 1 and 2, we show the comparison of various related physical parameters with two different forms carbon allotropes, diamond and graphite.

Name of Elements	Li	Be	B	C(Dia)	C(Graph
Atomic Number	3	4	5	6	6
Y(GPa)	11.5	289	440	1140	8.3
Melting Point (^{0}C)	181	1277	2030	3550	3550
Density (10^3 Kg/m^3)	0.531	1.85	2.34	2.25	2.25

Table 1: Comparison of Various physical parameters with diamond and graphite

Intuitively speaking, the materials with strong covalent bonds have a deep potential energy with a sharp curvature. Therefore, strong bonding naturally results in large values for Young's modulus. Similarly, the shallow potential well of the weakly bonded materials is responsible for small values of *Y* as evident above from table 1. Elements beyond carbon do not form solids with a three dimensional network of covalent bonds. For example, graphite having two dimensional sheet held together by van der Waals bonds possess a very small value of *Y* (about 8 GPa). Again, the interatomic distance varies with crystal direction in a solid along with corresponding variation of bond strength. This results an elastic anisotropy as a function of crystal direction. More importantly, this effect is prominent for those materials having two types of bonds. As an illustration, *Y* for

graphite in a direction parallel to the sheets is 950 GPa which is sensibly larger than that averaged over all direction (about 8 GPa). This picture is valid at absolute zero temperature.

Name of Elements	Na	Mg	Al	Si
Atomic Number	11	12	13	14
Y(GPa)	8.9	44	71	103
Melting Point (^{0}C)	98	650	660	1410
Density (10^3 Kg/m^3)	0.97	1.74	2.70	2.33

Table 2: Comparison of Various physical parameters of Alkali metals and Si

2. Computation of Young's Modulus

We begin the section with the definition of Young's modulus. It is defined as the ratio of longitudinal stress to longitudinal strain within elastic limit. Within elastic limit, the elongation (x) is proportional to the applied force (F) according to Hooke's law. This gives us the force constant (k) as the ratio of F to x. We would like to compute the Young's modulus of the material within this elastic limit of the chemical bond so called as harmonic approximation. If l_0 is the stress free length, A is the cross sectional area, we can write the Young's modulus as

$$Y = \frac{kl_0}{A} \qquad (1)$$

It is to be noted that the force constant k is related to the force between pair of atoms as

$$k = -\left[\frac{d^2U}{dr^2}\right]_{r=R_0} \quad \text{with} \quad F = -\frac{dU}{dr}.$$ Now, in the macroscopic specimen of length l_0 and cross-sectional area A, the specimen has roughly l_0/r_0 number of bonds where R_0 is the typical equilibrium distance of the interaction potential U(r). If one stretches this specimen by an infinitesimal distance dx, then the typical length of these bonds will increase by $\frac{R_0 dx}{l_0}$. Naturally, the tension in the each chain of atoms will be $\frac{kR_0 dx}{l_0}$. But the specimen contains $\frac{A}{R_0^2}$ of these chain of atoms, hence, the total force needed to produce an extension dx will be $\frac{kAdx}{l_0 R_0}$. Thus, the stress developed in the specimen is simply $\frac{kdx}{l_0 R_0}$. Therefore, the Young's modulus can be written in terms of force constant k as

$$Y = \frac{1}{R_0}\left[\frac{d^2U}{dr^2}\right]_{r=r_0} \qquad (2)$$

We model the potential of the chemical bonds by four different functions often taken in solid state physics. The first one in this category is the famous (6-12) Lennard-Jones potential given by

$$U_1(r) = U_0\left[\left(\frac{R_0}{r}\right)^{12} - 2\left(\frac{R_0}{r}\right)^6\right] \qquad (3)$$

This potential is also used in statistical mechanics and liquid state theory. The power 6 is due to the fluctuating dipolar interaction energy [13] while the power 12 is not fixed in the sense that it could be any power greater than 6 for the stability reason. In the fluctuating dipolar theory [13], it is assumed that the two atoms are separated by a distance *r*. If the instantaneous dipole moment of

the first atom is $\vec{p}_1$, then within the dipole approximation, the electric field at a distance r will scale as $\dfrac{\vec{p}_1}{r^3}$. As a result this field will eventually induce a dipole moment $\vec{p}_2$ in the second atom of the order of $\dfrac{\vec{p}_1}{r^3}$. Therefore, the typical fluctuating dipolar energy will be of the order $\dfrac{\vec{p}_1 \cdot \vec{p}_2}{r^3} \cong \dfrac{\vec{p}_1^2}{r^6}$. Interestingly, although the time average value of $\vec{p}_1$ and $\vec{p}_2$ is zero but the time average of interaction energy is non-zero because of the quadratic dependence on $\vec{p}_1$. It is interesting to note that the potential goes to zero in the asymptotic limit of the distance. Moreover, the force generated from the above interaction is restoring one because above the equilibrium distance R_0, the force is attractive and below R_0, repulsive in nature. We expand the force around the equilibrium distance $(r = R_0 + x_0)$ and restricting to linear elastic limit, we find

$$F = -\frac{72U_0}{R_0^2} x_0 = -kx_0 \qquad (4)$$

This helps to identify the relevant force constant (*k*). Hence, the Young's modulus can be written as

$$Y = \frac{288U_0}{\pi a d^2} \qquad (5)$$

Here, we have used $R_0 = a$ and the cross-sectional area $A = \dfrac{\pi d^2}{4}$ with d being the relevant diameter. One can also give a simple justification to the above formula from simple dimensional analysis [14]. Given the parameters used in the potential i.e. U_0 and R_0, it is easy to note that $Y \propto \dfrac{U_0}{R_0^3}$.

The expression obtained in equation (4) can now be used to estimate the typical magnitude of Young's modulus of CNT. Assuming $U_0 = 4.93$ eV as noted in case of Morse potential [15], we find the typical magnitude of force constant as 2790 N/m. For (9,0) SWCNT (the circumference turns out to be 2.2 nm), the equation (4) should be multiplied by 9 for the computation of Y. The estimated value thus turns out as 9363 GPa. This value is around 7.5 times larger than the experimentally observed value. The large value of U_0 taken in the above calculation is the reason for this discrepancy. However, 0.5 eV value of U_0 gives us a reasonable value of 948 GPa. If we take typical value $(1.68 \times 10^{-21}$ J) used for Ar atoms [15], we get back a very low value of Y (20 GPa) for (9,0) SWCNT.

As a generalization of the above potential, we consider the following one:

$$U(r) = U_0 \left(\frac{mn}{n-m} \right) \left[\frac{1}{m} \left(\frac{R_0}{r} \right)^m - \frac{1}{n} \left(\frac{R_0}{r} \right)^n \right] \qquad (6)$$

with $m. > n$. The equation (3) follows from the above equation in the limit $m = 12$ and $n = 6$. With this generalized potential, the expression for Y turns out as

$$Y = \frac{4mnU_0}{\pi a d^2} \qquad (7)$$

Another potential energy often used in molecular physics [16] is defined as

$$U_2(r) = B \left[\frac{R_0^7}{8r^8} - \frac{1}{r} \right] \qquad (8)$$

with $B = 2.31 \times 10^{-28}$ Jm. The second term in the above equation is the Coulomb term. In this case, the value of Y in terms of B becomes

$$Y = \frac{28B}{\pi a^2 d^2} \qquad (9)$$

When three positive charge particles are maintained in a straight line with the end particles being identical and are held fixed at a distance R_0, a new type potential [16] emerges

$$U_3(r) = B\left[\frac{1}{r} - \frac{1}{r - 2R_0}\right] \qquad (10)$$

The above elastic limit calculation yields the Young's modulus as

$$Y = \frac{16B}{\pi a^2 d^2} \qquad (11)$$

Another variant of anharmonic potential

$$U_4(r) = \left[-\frac{A_0}{r} + \frac{B_0}{r^9}\right] \qquad (12)$$

in material science [17] can also be used for rough estimation of Y. With $A_0 = 7.68 \times 10^{-29}$ Jm, it is easy to notice that the expression of $\frac{d^2 U_4}{dr^2}$ at the equilibrium distance (r_0) becomes

$$\frac{d^2 U_4(r_0)}{dr^2} = -\frac{2A_0}{r_0^3} + \frac{90B_0}{r_0^{11}} \qquad (13)$$

with $B_0 = \frac{A_0 r_0^8}{9}$. Therefore, the numerical value of Y for (9,0) becomes 825 GPa comparable to experimental observation.

The above picture is valid for absolute zero temperature. A suitable generalization to finite temperature can be done in the following way. At finite higher temperature, with the help of thermal energy, the atoms vibrate about their mean equilibrium positions. As a result, the amplitude of

the vibration increases with increase of temperature. With further increase of temperature (still quite far away from their respective melting points), the bonds between the atoms loosened up. As a consequence, there is a decrease of Young's modulus with temperature. With the help of linear expansion coefficient α, the expression (6) can be written at finite non-zero temperature as

$$Y(T) = \frac{4mnU_0}{\pi a_0(1 + \alpha T)d_0^2(1 + \alpha T)^2} \approx \frac{4mnU_0}{\pi a_0 d_0^2(1 + 3\alpha T)} \qquad (14)$$

In other words, the zero temperature and finite temperature Young's modulus are related roughly by

$$Y(T) \approx \frac{Y(0)}{1 + 3\alpha T} \qquad (15)$$

2. Computation of Tensile Strength

It is clear that for the computation of tensile strength, one has to take the single C-C bond in the hexagonal network. However, in all the above potentials, there is no information about the rupturing of the bond itself. However, we use the harmonic approximation to estimate the magnitude of the ultimate tensile strength in the following way. In Fig. 5, we show the variation of the scaled van der Waal interaction with scaled distance and the harmonic approximation adopted in it. The maximal elongation (x_{max}) is computed by equating the maximum potential energy at this distance to the bond energy. This gives us

$$x_{max} = \sqrt{\frac{2U_0}{k}} \qquad (16)$$

for the first potential in equation (3).

Therefore, the final maximum tensile strength in terms of Y can be written as

$$\sigma_{max} = \frac{Y x_{max}}{a} = \frac{Y}{6} \qquad (17)$$

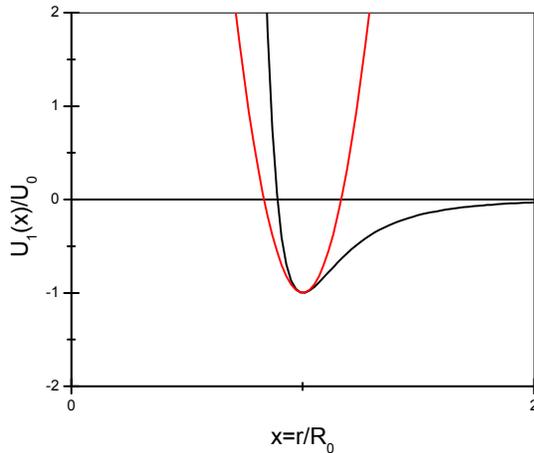$$\sigma_{max} = \frac{Y}{2} \qquad (19)$$

Fig. 5. Sketch of the scaled typical van der Waal interaction (black) and its harmonic approximation (red) with dimensionless distance

For (9,0) SWCNT, this value is simply 1560.5 GPa quite large compared to experimental observed value. Similar analysis for generalized Lennard –Jones potential in equation (6) yields the maximal value of tensile strength as

$$\sigma_{max} = Y \sqrt{\frac{2}{mn}} \qquad (18)$$

The equation (14) can also be used to estimate Y if σ_{max} of the material composing the system is known.

Fig. 6 represents the schematic variation of the interaction used in equation (8) with scaled distance. Please note the long tail of the interaction due to Coulomb interaction in contrast to Fig. 5. For the potential in equation (8), the ultimate tensile strength reduces to
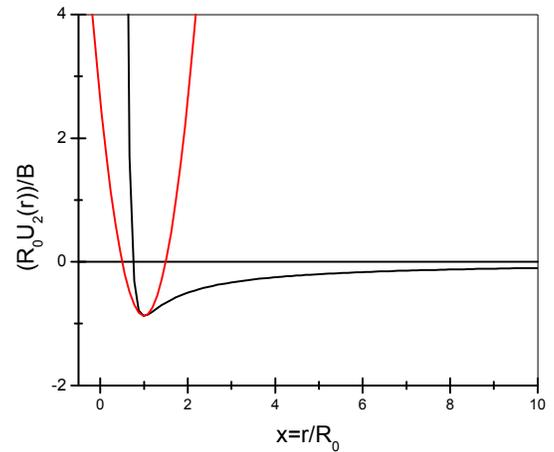

Fig. 6. Sketch of the scaled second interaction potential (black) used in equation (8) and its harmonic approximation (red) with dimensionless distance

Similarly, the expression for the potential given in equation (10) is recast as

$$\sigma_{max} = \frac{Y}{2} \qquad (20)$$

It should be remembered that the discrepancy arises in the large estimated values lies with the validity of harmonic approximation in such a situation. In fact, the harmonic approximation breaks down for rupturing the bonds in SWCNT.

In Table 3, we compare the different values of Y and σ_{max} obtained from all the above interaction potential with other observed values. The large difference between the theoretical predicted values and real experimental values may be due to structural defects inherent in SWCNT [15].

Table 3: Comparison of values of Young's modulus and tensile strength of (9,0) SWCNT

	Expt	Morse	U_1	U_2	U_3	U_4
(9,0) SWCNT Y (GPa)	270-950	1000	9533 948(*)	1872	1071	825
(9,0) SWCNT σ_{max} (GPa)	20-130	500	1560.5 158(*)	936	1071	389

Before we conclude we would like to point the possibility or prospect of carbon nanotubes as a space elevator [15, 18]. Till date CNT has not been produced at the macroscopic scale to produce a very long cable/rope connecting earth and space station/satellite. There might be occurrence of damage from atmosphere by storms and lightning. One has also to be careful to take appropriate precautions from collisions rendered by heavenly bodies moving around earth. Therefore, we still believe that its status as a space elevator remains in the arena of science fiction.

3. Conclusions

Within the limit of harmonic approximation, we have made a rough estimation of the Young's modulus and tensile strength of typical carbon nanotubes at zero temperature following four important potentials used in solid state physics. The theoretical results are compared with experimental observations. We have also generalized the zero temperature result to finite non-zero temperature with the help of linear expansion parameter. The results thus obtained

also find an important connection with the applicability of carbon nanotubes as a space elevator.

References :

[1] C. Binns, *Introduction to Nanoscience and Nanotechnology* (Wiley, NJ, 2010).
[2] D. Das, K. Nandi and D. Jana, Physics Education, **19**, No. 3, 155 (2002).
[3] S. Iijima, *Nature*, **354**, 56 (1991).
[4] S.Reich, C. Thomsen, J. Maulzsch, *Carbon nanotubes: basic concepts and physical properties* (Weinheim: Wiley-VCH; 2004).
[5] J. M. Schnorr, T. M. Swager, Chem Mater, **23**, 646 (2011).
[6] M. I. Katsnelson, Mater Today, **10**, 20 (2007).
[7] D. Jana, C.-L. Sun, L.-C. Chen, K.H. Chen, *Prog. Mat .Science*, **58**, 565 (2013).
[8] D. Jana, L.-C. Chen, C.W. Chen, S. Chattopadhyay, K.H. Chen, *Carbon*, **45**, 1482 (2007).
[9] J. C. Meyer et al., *Nano Lett*., **8**, 3582 (2008).
[10] A. K. Geim and K. S. Novoselov, *Nature Materials*, **6**, 183 (2007).
[11] K. S. Novoselov et al., *Nature*, **438**, 201 (2005).
[12] K. S. Novoselov et al., *Science*, **306**, 666 (2004
[13] N. W. Ashcroft and N. D. Mermin, *Solid State Physics* (Thomson, 2007).
[14] D. Jana, *Dimensional Analysis: Modern Perspectives* (Published by Lambert Academic Publishing, Germany, 2011).
[15] Z. Bochnicek, *Physics Teacher,* **51**, 462 (2013).

[16] H. D. Young and R. A. Fredman, *University Physics* (Pearson Education, 2004, India).

[17] M. S. Rogalski and S. B. Palmer,*Solid State Physics* (Gordon and Berach Science Publications, 2001).

[18] P. K. Aravind, *Am. J. Phys*., **75**, 125 (2007).